Çanakkale Onsekiz Mart University

Journal of Advanced Research in Natural and Applied Sciences

dergipark.org.tr/tr/pub/jarnas

Open Access

e-ISSN: 2757-5195 2024, Vol. 10, Issue 3, Pages: 587-600 doi.org/10.28979/jarnas.1448999

Particle Shape-Based Evaluation of the Leaching of Sphalerite Ore in Dilute Acid Solutions

Tuğba Deniz Tombal[1], İlgin Kurşun[2], Mert Terzi[3]

[1]Department of Mining Engineering, Faculty of Engineering, Adana Alparslan Türkeş Science and Technology University, Adana, Türkiye

[2,3]Department of Mining Engineering, Faculty of Engineering, İstanbul University-Cerrahpaşa, İstanbul, Türkiye

Article Info

Received: 12 Mar 2024

Accepted: 21 Jun 2024

Published: 30 Sep 2024

Research Article

Abstract − In this study, the effects of changes in particle shapes on dissolution efficiencies in zinc (Zn) recovery from a lead-zinc (Pb-Zn) ore by acid leaching method were investigated. In the experiments with nitric acid (HNO_3), sulfuric acid (H_2SO_4), and hydrochloric acid (HCl), particle size (75-106-150 µm), solids ratio (5-10-15-20-25%), leaching time (30-60-120-180-240 min), acid dosage (0.25-0.5-1-2-5 M) and pulp temperature (30-40-50-60-70 ºC) parameters were analyzed. Optimum results were obtained under the conditions of 75 µm particle size, 15% solids ratio, 120 min leaching time, 0.5 M acid dosage, and 50°C pulp temperature for H_2SO_4; 106 µm particle size, 25% solids ratio, 60 min leaching time, 0.5 M acid dosage, and 70°C pulp temperature for HCl; 75 µm particle size, 20% solids ratio, 60 min leaching time, 1 M acid dosage, and 50°C pulp temperature for HNO_3. As a consequence of the tests performed under these optimized conditions, 97.32%, 96.38% and 96.06% Zn dissolution efficiencies were obtained. Within the context of particle shape factor research, microscope images of the leaching residues were obtained from the experiments in which the pulp temperature, acid dosage, and leaching time parameters were examined. The samples obtained from the experiments with all three acids were compared with the ore samples, and the impacts of changes in circularity, roundness, and solidity values on dissolution efficiencies were interpreted.

Keywords − *Sphalerite, chemical dissolution, particle shape factor analysis*

1. Introduction

Morphology is a common term for the detailed description of an object and is considered to have two main sides: shape and surface texture. Shape relates to large and medium-scale aspects of an object's morphology, while surface texture refers to small-scale surface features related to the object's size. Particle morphology, including size and shape, is an important factor that significantly affects the physical and chemical properties of the material. Basic information about the nature and origin of granular material can often be obtained from the particles' shape, form, and/or surface shape [1-3]. Shape is a basic characteristic of all objects, even sedimentary particles, but it remains one of the most challenging processes to measure and characterize. Despite a huge bibliography on the topic, there continues to be a pervasive misunderstanding about the importance and relative value of various measurements of particle shape. Different researchers have used various terms to describe the external geometric expression of particles, including shape, morphology, and form. While several shape dimensions can be defined, four are particularly important: form, roundness, roughness, and sphericity [4-7].

[1]ttombal@atu.edu.tr (Corresponding Author); [2]ilginkur@iuc.edu.tr; [3]mert.terzi@iuc.edu.tr

Particle circularity is a measure of the extent to which the shape of a particle resembles a circle. This dimensionless value ranges from 0 to 1, with 1 indicating a perfect circle. The circularity of a particle is calculated from the ratio of the area of the particle projection to its circumference. A rough particle surface leads to low numerical values of the circularity parameter. The particle circularity is one of the most common shape factors used in particle analysis [8, 9]. Roundness is a measure of the extent to which the corners and edges of a particle are eroded. Particle roundness is also an important aspect of particle morphology and is directly related to granular materials' mechanical response and strength [10, 11]. Particle solidity, one of the parameters used to characterize the shape of particles, is a measure of the overall concavity of a particle. It is described as the ratio of a particle's area to its convex body's area. Solidity is a dimensionless value ranging from 0 to 1; 1 indicates a completely hard object with no concavity, while 0 indicates an object with infinite concavity. Solidity is used to evaluate particles' performance and understand their physical properties [12].

Leaching processes play an important role in industries ranging from mining to environmental remediation. The efficiency of leaching processes depends on several factors, including particle size, surface area, and particle shape. While great emphasis has been placed on particle size and surface area, the importance of particle shape in leaching remains a topic of debate and research. One of the key factors affecting leaching kinetics is the surface area of solid particles. It is assumed that particles with larger surface area have more contact with the leaching solution, resulting in faster leaching. However, the role of particle shape complicates this relationship. Irregularly shaped particles may have higher surface areas than spherical particles of similar size, potentially enhancing leaching kinetics.

In contrast, sharp edges and crevices in irregularly shaped particles can impede mass transfer, leading to non-uniform leaching and lower efficiencies. Particle shape can also influence the hydrodynamics of the leaching system, affecting the transport of reactants and products to the particle surface and the distribution of the leach solution around the particles. Irregularly shaped particles can lead to inhomogeneous leaching behavior. Despite advances in modeling and simulation techniques, accurately predicting the behavior of irregularly shaped particles in leaching processes remains a significant challenge [13-16].

The purpose of this study is to understand how the morphology of ore particles impacts the leaching process and to determine how it affects the efficiency when exposed to dilute sulfuric acid (H_2SO_4), hydrochloric acid (HCl), and nitric acid (HNO_3) solutions while optimizing the leaching process by determining the most effective conditions to maximize zinc (Zn) extraction. In this context, controlled leaching experiments with varying parameters were conducted to determine optimum dissolution. Additionally, the effect of particle shape on leaching kinetics was evaluated by microscopy investigations to analyze the circularity, roundness, and solidity factors of sphalerite ore particles. Moreover, the relationship between particle shape and the efficiency of sphalerite dissolution in dilute acid solutions was investigated. Based on the results obtained from this study, the effects of particle shape factor on leaching efficiency were examined to shed light on future studies.

2. Materials and Methods

The representative samples used in this study were taken from Esan Eczacıbaşı Inc. Balya Lead-Zinc plant located in the Balya district of Balıkesir province, Türkiye. First, the number of representative samples weighing approximately 100 kg was reduced using coning-quartering and sample grid methods. Then, the size reduction was performed gradually using a jaw crusher (Baz Machinery, Türkiye). Finally, the samples crushed below 2 mm were ground using a ball mill-sieve closed circuit system to the appropriate size for leaching experiments. An agate mortar (Retsch, RM 200, Germany) was used for sample preparation for elemental analysis and density experiments. Moisture analysis was performed in an oven (Memmert, Uf450) at 105°C to characterize the sample's moisture content. Density experiments were carried out in 50 ml pycnometers using distilled water. Moisture and density analyses were performed according to American Society for Testing and Materials (ASTM) standards. As a result of the experiments, the moisture value was 0.069%, and the density value was 4.89 g/cm^3. Particle size analysis was performed using the wet sieving method with the Retsch sieve series. According to the results of the particle size analysis of the sample, the d_{10}, d_{50}, and d_{80} dimensions of the sample were found to be 0.21 mm, 1.4 mm, and 3.55 mm, respectively. Inductively coupled plasma optical emission spectroscopy (ICP-OES) analysis revealed that the sample contained 2.14% Zn. ICP-OES analyses were carried out at the Department of Mineral Analysis and Technology, General Directorate of Mineral Research and Exploration.

Within the scope of mineralogical studies, X-Ray Diffraction (XRD) analysis (Rigaku, MiniFlex 600, Japan) was first performed, and it was observed to contain quartz, dolomite, albite, and sphalerite. Sphalerite (ZnS), low amounts of galena (PbS), and trace amounts of pyrite (FeS_2) were observed in the sample within the scope of polished section studies. Galena formations are observed in fractured formations, non-euhedral, and isotropic. Limestone is observed in an anisotropic form as gangue minerals to represent the waste rock. Apart from limestone, iron sulfides are also observed as inclusions in the gangue as small pseudomorphs.

The effect of H_2SO_4, HCl, and HNO_3 leaching processes on the dissolution efficiency of Zn recovery was investigated within the scope of leaching experiments. The pH values were checked periodically during the experiments, and a variation of $< \pm 0.1$ was observed. For the leaching experiments, 98% pure H_2SO_4 (Sigma-Aldrich), 37% pure HCl (Sigma-Aldrich), and 55% pure HNO_3 (Sigma-Aldrich) were used. Solid-liquid separation after leaching experiments was carried out using Whatman (4 µm) filter papers. The leaching tailings obtained after solid-liquid separation were washed with 1% acid solution in 2 stages, and then Zn contents were analyzed by the Inductively coupled plasma mass spectrometry (ICP-MS) method. The dissolution efficiency was calculated according to (2.1):

$$\%\,Efficiency = \frac{Zn\,(in\,run-of-mine) - Zn(in\,tailings)}{Zn(in\,run-of-mine)} * 100 \tag{2.1}$$

The following reactions (2.2)-(2.4) are thought to occur during leaching processes [17-19]:

$$ZnS + H_2SO_4 + {}^{1}/_{2}\,O_2 = ZnSO_4 + H_2O + S \tag{2.2}$$

$$ZnS + 2HCl_{(aq)} = ZnCl_{2(aq)} + H_2S \tag{2.3}$$

$$ZnS_{(s)} + 8HNO_{3(aq)} = Zn^{2+}_{(aq)} + SO^{2-}_{4(aq)} + 8NO_{2(g)} + 4H_2O \tag{2.4}$$

In the leaching experiments, the effects of solvent concentration, pulp temperature, solids ratio, dissolution time, and particle size parameters on the dissolution of the sample were examined, and the optimum values for each parameter were determined.

Within the scope of the particle shape factor studies, at least 10 photographs were taken with a digital microscope (IronX). At least 300 data were collected for each run-of-mine sample and the leachate sample to be analyzed for shape factors. The total counted particle number was within the range of previous studies where the particles were counted manually [20].

These photographs were then analyzed through the ImageJ program, and the average values of circularity, roundness, and solidity were determined by the data obtained from all photographs. Then, microscope photographs were taken of the leach samples from the experiments in which the pulp temperature, acid dosage, and leaching time parameters were tested, and the optimum values were determined. The values obtained from the ore sample were compared with those obtained from the leachate samples, interpreted by utilizing the data in Tables 1 and 2, and the effects of changes in particle shapes on dissolution efficiency were revealed.

Table 1. [7] Alternative roundness classification schemes based on Wadell's [21] measurement method

	Russel and Taylor [22]		Pettijohn [23]		Powers [24]		Blott and Pye [7]	
	CL	AM	CL	GM	CL	GM	CL	GM
Very Angular	-	-	-	-	0.12-0.17	0.14	-	
Angular	0.00-0.15	0.075	0.00-0.15	0.125	0.17-0.25	0.21	0-0.13	0.09
Sub-angular	0.15-0.30	0.225	0.15-0.25	0.200	0.25-0.35	0.30	0.13-0.25	0.18
Sub-rounded	0.30-0.50	0.400	0.25-0.40	0.315	0.35-0.49	0.41	0.25-0.50	0.35
Rounded	0.50-0.70	0.600	0.40-0.60	0.500	0.49-0.70	0.59	0.50-1.00	0.71
Well rounded	0.70-1.00	0.850	0.60-1.00	0.800	0.70-1.00	0.84	-	

CL: Class limits, AM: Arithmetic Mean, GM: Geometric Mean

Table 2. [7] Proposed classification scheme for particle circularity (when used in two dimensions) or particle sphericity (when applied in three dimensions), measured using the method of Riley [25]

	CL	GM
Very high circularity/sphericity	0.894-1.000	0.949
High circularity/sphericity	0.775-0.894	0.837
Moderate circularity/sphericity	0.632-0.775	0.707
Low circularity/sphericity	0.447-0.632	0.548
Very low circularity/sphericity	0.000-0.447	0.316

3. Results and Discussion

The parameter ranges tested in the leaching experiments, the dissolution efficiencies and the optimum parameters are presented in Table 3. The dissolution efficiencies in the experiments with all three acids were between 92.69% and 97.63%. The final highest dissolution efficiency was obtained in the experiment with H_2SO_4.

Table 3. Data of the leaching experiments

Acid	Experiment	Parameters	Dissolution Efficiency (%)	Optimum Parameter
H_2SO_4	Particle size (µm) (d_{100})	75, 106, 150	97.12	106
	Solids ratio (%)	5, 10, 15, 20, 25	97.27	15
	Leaching time (min)	30, 60, 90, 120, 180, 240	96.25	120
	Acid dosage (M)	0.25, 0.5, 1, 2, 5	97.63	0.5
	Pulp temperature (ºC)	30, 40, 50, 60, 70	97.32	50
HCl	Particle size (µm) (d_{100})	75, 106, 150	95.59	106
	Solids ratio (%)	5, 10, 15, 20, 25	96.56	25
	Leaching time (min)	30, 60, 90, 120, 180, 240	92.69	60
	Acid dosage (M)	0.25, 0.5, 1, 2, 5	95.90	0.5
	Pulp temperature (ºC)	30, 40, 50, 60, 70	96.38	70
HNO_3	Particle size (µm) (d_{100})	75, 106, 150	93.24	75
	Solids ratio (%)	5, 10, 15, 20, 25	96.44	20
	Leaching time (min)	30, 60, 90, 120, 180, 240	93.09	60
	Acid dosage (M)	0.25, 0.5, 1, 2, 5	97.21	1
	Pulp temperature (ºC)	30, 40, 50, 60, 70	96.06	50

Since the optimum values for the leaching experiments were obtained at particle sizes of 106 µm and 75 µm, firstly, microscope photographs were taken of the samples with these particle sizes (Figure 1). The average particle shape factor value (AV), standard deviation (SD), minimum (Min), and maximum (Max) values for the roundness, circularity, and solidity values of each sample were calculated by performing particle shape factor analysis using ImageJ analysis program (Table 4).

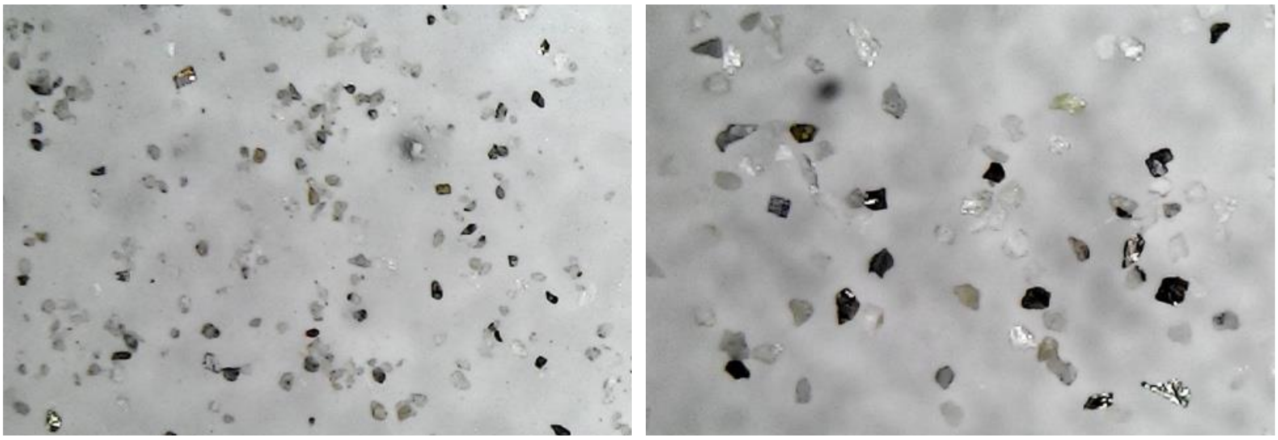

(1) 106 µm (2) 75 µm

Figure 1. Microscope photographs of the run-of-mine samples

Table 4. Results of ImageJ analysis of run-of-mine samples

	Circularity				**Roundness**				**Solidity**			
	AV	**SD**	**Min**	**Max**	**AV**	**SD**	**Min**	**Max**	**AV**	**SD**	**Min**	**Max**
(1)	0.633	0.211	0.161	0.998	0.650	0.164	0.162	0.989	0.808	0.101	0.448	0.974
(2)	0.525	0.228	0.086	0.917	0.649	0.171	0.170	0.969	0.776	0.138	0.366	0.952

Subsequently, the leaching residual samples for which optimum values were obtained for the pulp temperature, acid dosage, and leaching time experiments where dissolution efficiencies were examined were photographed, and particle shape factor analysis was performed using the ImageJ analysis program. The AV, SD, Min, and Max values of each sample's roundness, circularity, and solidity values were calculated. The results obtained were compared with the data from the run-of-mine samples, and the effects of particle shape factor on dissolution kinetics were attempted to uncover. Table 5 shows the codes assigned to the samples for each experiment within the scope of particle shape factor studies.

Table 5. The codes assigned to the samples for each experiment within the scope of particle shape factor studies

Sample code	**Experiment**
$Zn_{ltH2SO4}$	Leaching time (H_2SO_4)
$Zn_{adH2SO4}$	Acid dosage (H_2SO_4)
$Zn_{ptH2SO4}$	Pulp temperature (H_2SO_4)
Zn_{ltHCl}	Leaching time (HCl)
Zn_{adHCl}	Acid dosage (HCl)
Zn_{ptHCl}	Pulp temperature (HCl)
Zn_{ltHNO3}	Leaching time (HNO_3)
Zn_{adHNO3}	Acid dosage (HNO_3)
Zn_{ptHNO3}	Pulp temperature (HNO_3)

The results obtained by photographing the leaching samples (Figure 3, Figure 5, Figure 7) of the optimum values acquired as a result of the tests performed with H_2SO_4, HCl, and HNO_3 at various value ranges for pulp temperature, acid dosage, and leaching time parameters, and analyzing the particle shape factor in ImageJ analysis program were presented in Table 6.

Table 6. ImageJ analysis results of optimum leaching residual samples

	Circularity				Roundness				Solidity			
	AV	**SD**	**Min**	**Max**	**AV**	**SD**	**Min**	**Max**	**AV**	**SD**	**Min**	**Max**
$Zn_{ltH2SO4}$	0.613	0.193	0.134	0.914	0.709	0.151	0.286	0.949	0.848	0.083	0.579	0.943
$Zn_{adH2SO4}$	0.621	0.199	0.168	0.926	0.694	0.151	0.288	0.974	0.821	0.098	0.557	0.953
$Zn_{ptH2SO4}$	0.619	0.222	0.072	0.976	0.687	0.150	0.279	0.981	0.816	0.128	0.321	0.950
Zn_{ltHCl}	0.678	0.180	0.129	0.996	0.671	0.165	0.216	0.995	0.832	0.083	0.330	0.950
Zn_{adHCl}	0.622	0.219	0.126	0.985	0.639	0.173	0.173	0.977	0.805	0.110	0.439	0.971
Zn_{ptHCl}	0.605	0.226	0.121	0.988	0.648	0.170	0.059	0.989	0.790	0.123	0.363	0.967
Zn_{ltHNO3}	0.607	0.219	0.139	0.976	0.662	0.160	0.168	0.977	0.808	0.119	0.407	0.947
Zn_{adHNO3}	0.669	0.213	0.107	0.990	0.674	0.167	0.191	0.978	0.834	0.110	0.341	0.968
Zn_{ptHNO3}	0.620	0.212	0.142	0.994	0.649	0.162	0.200	0.984	0.795	0.103	0.327	0.952

3.1. Investigation of Leaching Residues of Experiments Performed with H_2SO_4

ImageJ analyses of the optimum leaching residual samples are shown in Figure 2; optical microscope photographs and ImageJ outputs are seen in Figure 3.

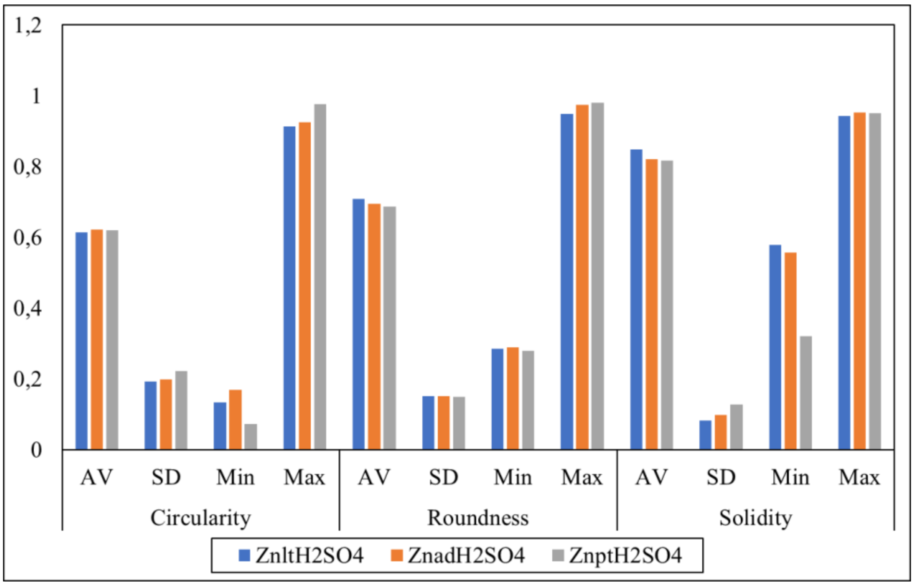

Figure 2. ImageJ analysis results of optimum leaching residual samples (Leaching time: 120 min, Acid dosage: 0.5 M, Pulp temperature: 50 °C)

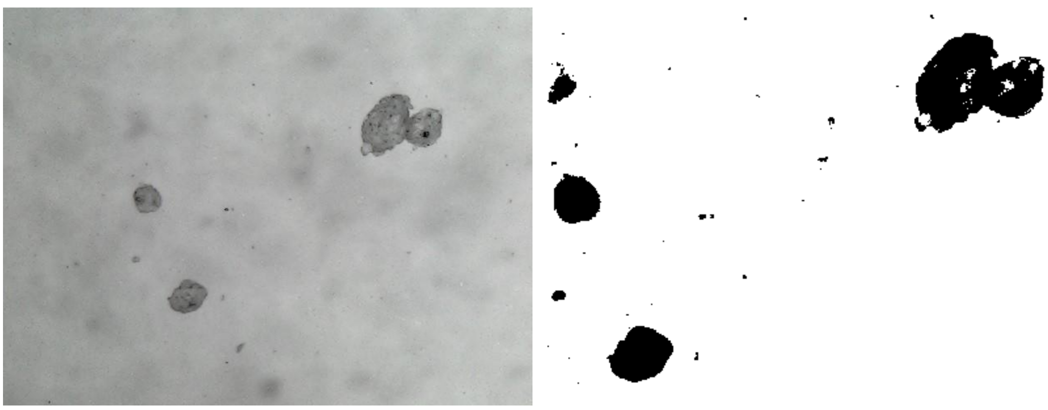

$Zn_{ltH2SO4}$ ImageJ output of $Zn_{ltH2SO4}$

(a)

Figure 3. Optical microscope photographs and ImageJ outputs of (a) $Zn_{ltH2SO4}$, (b) $Zn_{adH2SO4}$, and (c) $Zn_{ptH2SO4}$

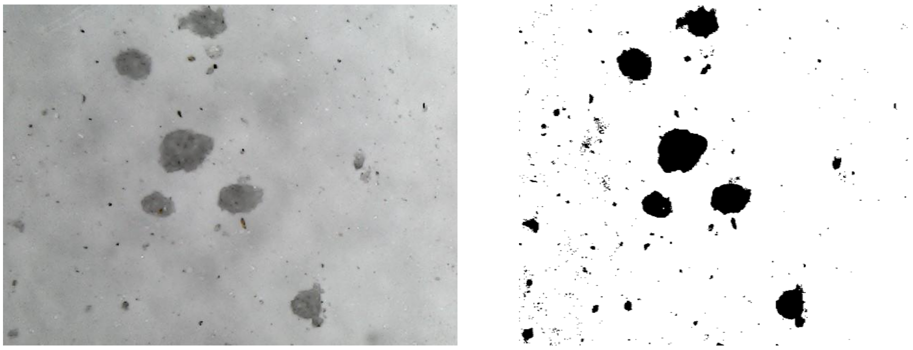

$Zn_{adH2SO4}$ ImageJ output of $Zn_{adH2SO4}$

(b)

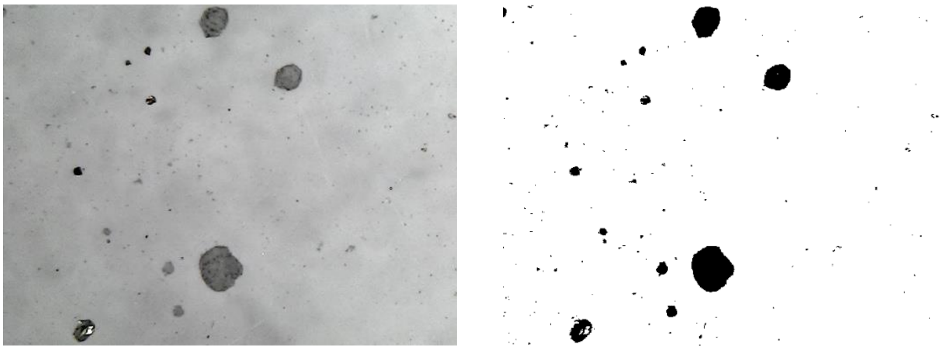

$Zn_{ptH2SO4}$ ImageJ output of $Zn_{ptH2SO4}$

(c)

Figure 3. (Continued) Optical microscope photographs and ImageJ outputs of (a) $Zn_{ltH2SO4}$, (b) $Zn_{adH2SO4}$, and (c) $Zn_{ptH2SO4}$

As a result of H_2SO_4 leaching, circularity values of all three samples decreased, while roundness and solidity values increased. According to the circularity values given in Table 2, all three samples were within the "low circularity" class limit. According to the roundness values given in Table 1, it was observed that the $Zn_{ltH2SO4}$ sample belonged to the "well-rounded" class limit according to Russel and Taylor [22], Powers [24], and Pettijohn [23] and to the "rounded" class limit according to Blott and Pye [7]. $Zn_{adH2SO4}$ and $Zn_{ptH2SO4}$ samples were found to be within the "rounded" class limit according to Russel and Taylor [22], Powers [24], and Blott and Pye [7], and within the "well rounded" class limit according to Pettijohn [23].

3.2. Investigation of Leaching Residues of Experiments Performed with HCl

ImageJ analysis results of the optimum leaching residual samples are given in Figure 4, and optical microscope photographs and ImageJ outputs are seen in Figure 5.

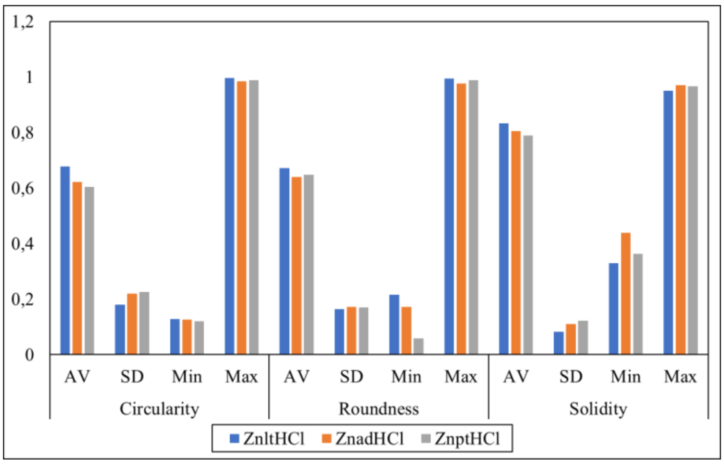

Figure 4. ImageJ analysis results of optimum leaching residual samples (Leaching time: 60 min, Acid dosage: 0.5 M, Pulp temperature: 70 ºC)

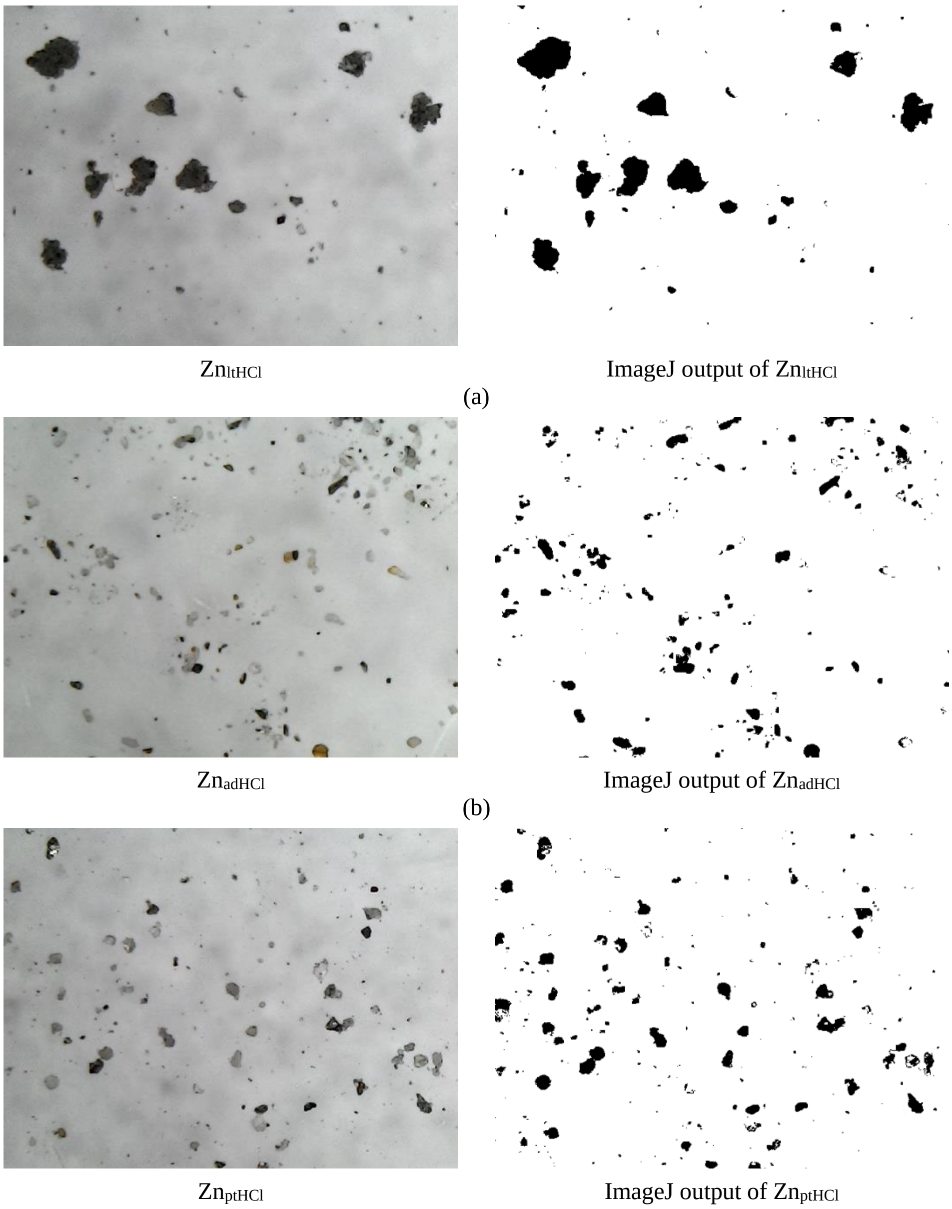

(c)

Figure 5. Optical microscope photographs and ImageJ outputs of (a) Zn_{ltHCl}, (b) Zn_{adHCl}, and (c) Zn_{ptHCl}

It was noticed that the circularity values of each of the three samples increased due to HCl leaching. While the roundness value of Zn_{ltHCl} increased, the roundness values of Zn_{adHCl} and Zn_{ptHCl} decreased. When the solidity values were analyzed, it was noticed that the solidity values of all three specimens significantly increased. According to the circularity values given in Table 2, the Zn_{ltHCl} sample was within the "moderate circularity" class limit, and the Zn_{adHCl} and Zn_{ptHCl} samples were within the "low circularity" class limits. According to the roundness values given in Table 1, it was found that Zn_{ltHCl}, Zn_{adHCl}, and Zn_{ptHCl} samples were included in the "rounded" class limit according to Russel and Taylor [22], Powers [24], and Blott and Pye [7], and in the "well rounded" class limit according to Pettijohn [23].

3.3. Investigation of Leaching Residues of Experiments Performed with HNO_3

ImageJ analysis results of the optimum leaching residual samples are shown in Figure 6, and optical microscope photographs and ImageJ outputs are seen in Figure 7.

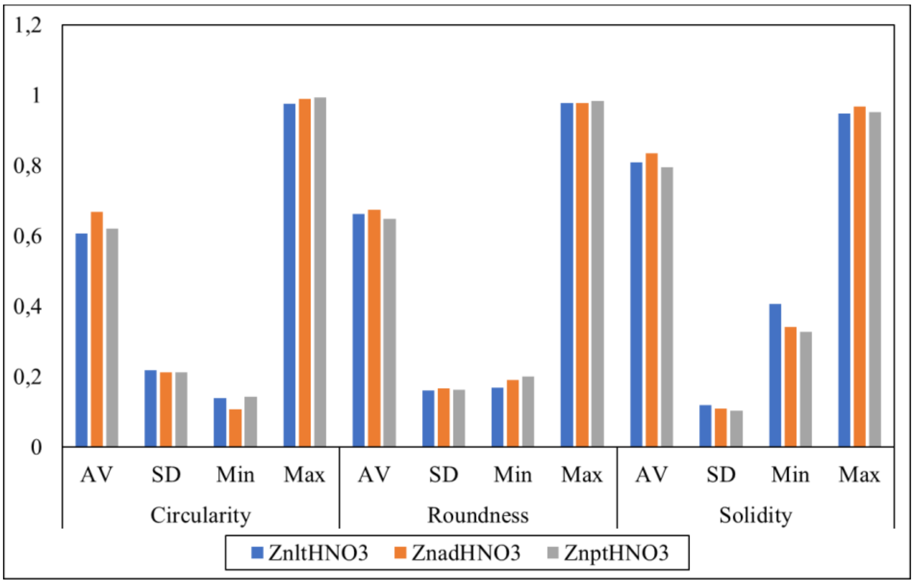

Figure 6. ImageJ analysis results of optimum leaching residual samples (Leaching time: 60 min, Acid dosage: 1 M, Pulp temperature: 50 ºC)

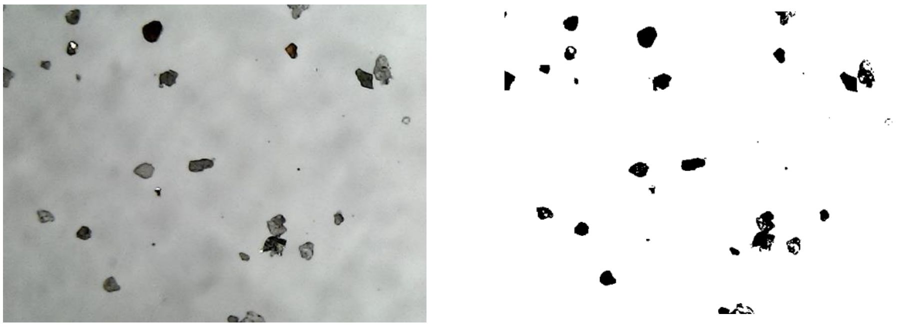

Zn_{ltHNO3} ImageJ outputs of Zn_{ltHNO3}

(a)

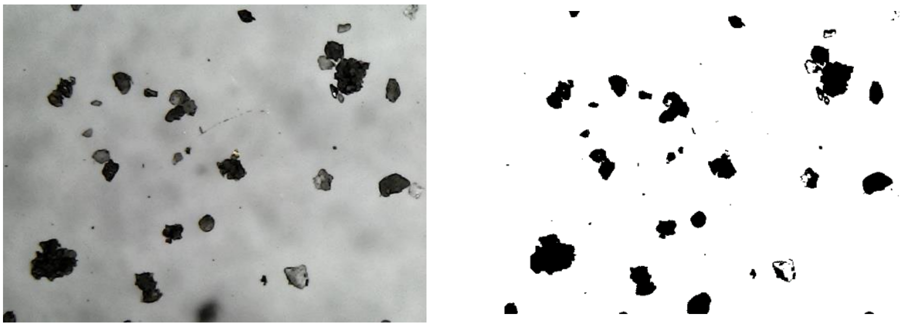

Zn_{adHNO3} ImageJ outputs of Zn_{adHNO3}

(b)

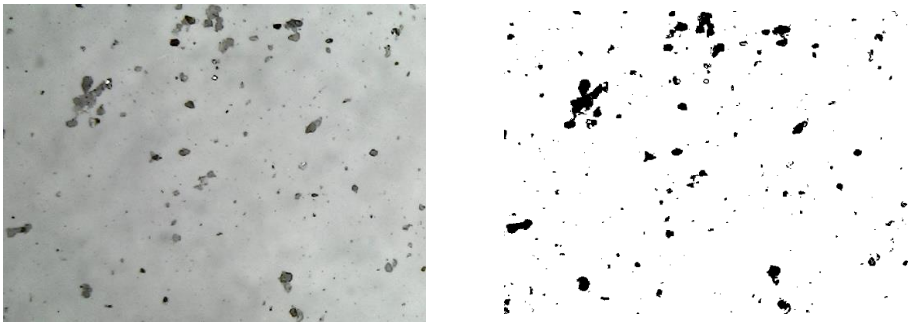

Zn_{ptHNO3} ImageJ outputs of Zn_{ptHNO3}

(c)

Figure 7. Optical microscope photographs and ImageJ outputs of (a) Zn_{ltHNO3}, (b) Zn_{adHNO3}, and (c) Zn_{ptHNO3}

As a result of HNO_3 leaching, the circularity values of the Zn_{ltHNO3} and Zn_{ptHNO3} samples decreased, but the circularity value of the Zn_{adHNO3} sample increased. Whereas the roundness values of Zn_{ltHNO3} and Zn_{adHNO3} samples increased, the roundness value of Zn_{ptHNO3} sample decreased. The solidity value of the Zn_{ltHNO3} sample had a stable value, but the Zn_{adHNO3} sample had an increased solidity value, and the Zn_{ptHNO3} sample had a decreased solidity value. According to the circularity values given in Table 2, it was seen that Zn_{ltHNO3} and Zn_{ptHNO3} samples were in the range of "low circularity" class limits, and the Zn_{adHNO3} sample was in the range of "moderate circularity" class limit. According to the roundness values given in Table 1, it was observed that Zn_{ltHNO3}, $Zn_{adHNO3,}$ and Zn_{ptHNO3} samples were within the "rounded" class limit according to Russel and Taylor [22], Powers [24], and Blott and Pye [7], and within the "well rounded" class limit according to Pettijohn [23]. The results of the particle shape factor studies are summarized in Table 7.

Table 7. The summary of particle shape factor studies

Experiment	Circularity	Roundness	Solidity	Based on Table 2	Russel and Taylor [22]	Pettijohn [23]	Powers [24]	Blott and Pye [7]
$Zn_{ltH2SO4}$	Decreased	Increased	Increased	Low circularity	Well rounded	Well rounded	Well rounded	Rounded
$Zn_{adH2SO4}$	Decreased	Increased	Increased	Low circularity	Rounded	Well rounded	Rounded	Rounded
$Zn_{ptH2SO4}$	Decreased	Increased	Increased	Low circularity	Rounded	Well rounded	Rounded	Rounded
Zn_{ltHCl}	Increased	Increased	Increased	Moderate circularity	Rounded	Well rounded	Rounded	Rounded
Zn_{adHCl}	Increased	Decreased	Increased	Low circularity	Rounded	Well rounded	Rounded	Rounded
Zn_{ptHCl}	Increased	Decreased	Increased	Low circularity	Rounded	Well rounded	Rounded	Rounded
Zn_{ltHNO3}	Decreased	Increased	Stable	Low circularity	Rounded	Well rounded	Rounded	Rounded
Zn_{adHNO3}	Increased	Increased	Increased	Moderate circularity	Rounded	Well rounded	Rounded	Rounded
Zn_{ptHNO3}	Decreased	Decreased	Decreased	Low circularity	Rounded	Well rounded	Rounded	Rounded

Sulfuric acid, hydrochloric acid, and nitric acid all belong to strong mineral acids. Despite differences in their chemical structures and properties, they share common functional groups (sulfonic, chloride, and nitrate groups, respectively) [26-28]. These functional groups probably determine similar interactions with the metal ore during dissolution, leading to comparable shape parameters. However, sulfuric, hydrochloric, and nitric acid's high reactivities can facilitate similar chemical processes during ore dissolution, resulting in dissolution residues with similar shapes and properties. This is due to these acids' strong oxidizing and complexing abilities, which enable them to effectively break down and dissolve various minerals and ore [29-35]. In this study, particle shape's effect on dissolution was observed in a limited manner due to the complex structure of the material. Therefore, it is recommended to carry out experimental studies on pure selected particles to eliminate the effect of heterogeneity in future studies.

The particle shape factor can influence the leaching mechanisms. For example, in the study by Ghorbani et al. on the progression of zinc leaching from large sphalerite ore particles, the authors found that the leaching mechanisms differed significantly between particles with different shapes. They observed that leaching from large particles led to near complete conversion near the surface but only partial conversion in the zones closer to the center of the particles. This suggests that the particle shape can influence the distribution of leaching agents and the reaction rates within the particles [36]. Another research study emphasized the significant role of particle shape in influencing transient fluid flow dynamics during particle adsorption and dispersion. This was highlighted through Particle Image Velocimetry (PIV) measurements, suggesting that different particle shapes could lead to varied fluid flow dynamics around the particles, which might influence the leaching rates and efficiencies [37]. This could be particularly relevant in processes where the interface between the particle surface and the leachate solution critically determines the overall reaction kinetics. This research highlights the importance of particle shape in Zn leaching experiments and suggests that further investigation is needed to understand its full implications for advanced plant applications. By investigating the effects of particle shape on dissolution efficiencies in zinc recovery through acid leaching, the study sheds light on an aspect of mineral processing that has not been extensively explored. By analyzing microscope images of leaching residues and comparing them with ore samples, the study provides insights into the impact of particle circularity, roundness, and solidity on dissolution efficiencies. This understanding can guide future research in particle morphology and its influence on various processes.

4. Conclusion

Particle roundness, circularity, and solidity can impact ore beneficiation processes, as they can affect particulate materials' behavior and the particles' surface properties. The decrease in particle roundness is thought to cause the particles to rotate less despite a higher displacement value, as stated in [38]. The study's findings supported the relationship between more spherical particles, shorter disintegration time and higher dissolution rate [39]. This is because, as stated in [40], it is thought that the specific surface area of the particle increases with decreasing particle size, leading to an increase in the dissolution rate. From these, it can be concluded that circularity may indirectly affect dissolution efficiency through its effect on particle size and surface area. Particle circularity and solidity can affect the homogeneity and quality of the final product. Particle solidity can significantly impact leaching by affecting the rate of chemical reactions, permeability, and infiltration.

Since particle morphology is still poorly understood to evaluate the success of chemical dissolution and intergranular interactions, it is necessary to identify, model, and determine the mechanisms affecting dissolution through various measurements in combination with chemical dissolution experiments and dissolution kinetics analysis. Although there is a wide range of shape factors, the main purpose of prioritizing the roundness, circularity, and solidity values in this study is to search the effect of particle shape on chemical dissolution processes by considering the changes in these values. When the results obtained were analyzed, it was seen that changes in particle shape could be a control factor in Zn leaching experiments. The study established the relationship between particle shape and leaching efficiency in a limited manner. It is recommended to carry out experimental studies on pure selected particles in milder conditions in order to eliminate the effect of heterogeneity and to see the particle-specific effects more clearly in future studies, as particle morphology is a process that still requires further research and development for advanced plant applications.

Author Contributions

The first author contributed to the experimental studies and writing of the manuscript. The second author contributed to the design of experimental studies, manuscript writing, and interpretation of findings. The third author contributed to the writing of the manuscript and interpretation of the findings. All authors read and approved the final version of the paper.

Conflicts of Interest

All the authors declare no conflict of interest.

Ethical Review and Approval

No approval from the Board of Ethics is required.

References

[1] Z. Lu, X. Hu, Y. Lu, *Particle morphology analysis of biomass material based on improved image*

processing method, International Journal of Analytical Chemistry Special issue (2017) Article ID 5840690 9 pages.

[2] Upstate Medical University, Particle Morphology (2018), http://www.upstate.edu/pathenvi/basics/particle_morphology.php, Accessed 30 Jan 2018.

[3] Chulalongkorn University, Particle Morphology (2018), http://www.geo.sc.chula.ac.th/courses/2307223/2307223_02-particle_morphology.pdf, Accessed 30 Jan 2018.

[4] A. R. Yudhbir, *Quantification of particle shape and angularity using the image analyzer*, Geotechnical Testing Journal 14 (3) (1991) 296–308.

[5] E. T. Bowman, K. Soga, T. W. Drummond, *Particle shape characterisation using Fourier Analysis*, Géotechnique 51 (6) (2001) 545–554.

[6] M. Uzuntaş, *Investigation of crusher type effect on the particle shape by image analysis method*, Master's Thesis Eskişehir Osmangazi University (2007) Eskişehir.

[7] S. J. Blott, K. Pye, *Particle shape: a review and new methods of characterization and classification*, Sedimentology 55 (1) (2008) 31–63.

[8] J. R. Grace, A. Ebneyamini, *Connecting particle sphericity and circularity*, Particuology 54 (2021) 1–4.

[9] U. Ulusoy, H. Kurşun, İ. Erdoğan, *Statistical significance testing of the particle circularity values from various products of sphalerite column flotation beneficiation with ultrasonic pretreatment*, in: A. İşman, Ş. Dündar (Eds.), International Science and Technology Conference, Berlin, 2017, pp.524–539.

[10] N. Roy, P. Vangla, J. D. Frost, G. M. Latha, *An enhanced automated particle angularity measurement method*, Journal of Testing and Evaluation 50 (2) (2021) 1060–1078.

[11] W. Wang, L. Xu, Z. Liu, R. Huang, Y. Lai, Y. Liu, D. Ruping, *Comparison and application of three quantitative methods to describe sedimentary particle shape*s, Geological Review (3) (2013) 553–562.

[12] L. E. Liem, D. Smith, S. J. Stanley, *Particle reduction study of flocculation mixing by means of grids*, Canadian Journal of Civil Engineering 26 (1999) 251–261.

[13] F. Faraji, A. Alizadeh, F. Rashchi, N. Mostoufi, *Kinetics of leaching: A review*, Reviews in Chemical Engineering 38 (2) (2022) 113–148.

[14] Y. Ghorbani, M. Becker, A. Mainza, J. P. Franzidis, J. Petersen, *Large particle effects in chemical/biochemical heap leach processes – A review*, Minerals Engineering 24 (11) (2011) 1172–1184.

[15] Y. Li, N. Kawashima, J. Li, A. P. Chandra, A. R. Gerson, *A review of the structure, and fundamental mechanisms and kinetics of the leaching of chalcopyrite*, Advances in Colloid and Interface Science 197–198 (2013) 1–32.

[16] J. MacCarthy, A. Nosrati, W. Skinner, J. Addai-Mensah, *Effect of mineralogy and temperature on atmospheric acid leaching and rheological behaviour of model oxide and clay mineral dispersions*, Powder Technology 286 (2015) 420–430.

[17] A. A. Baba, F. A. Adekola, *Hydrometallurgical processing of a Nigerian sphalerite in hydrochloric acid: Characterization and dissolution kinetics*, Hydrometallurgy 101 (2010) 69–75.

[18] M. Çopur, *Solubility of ZnS concentrate containing pyrite and chalcopyrite in HNO3 solutions*, Chemical and Biochemical Engineering Quarterly 15 (4) (2001) 181–184.

[19] R. J. Jan, M. T. Hepworth, V. G. Fox, *A kinetic study on the pressure leaching of sphalerite*, Metallurgical Transactions B 7B (1976) 353–361.

[20] W. Yin, Z. Zhu, B. Yang, Y. Fu, J. Yao, *Contribution of particle shape and surface roughness on the*

flotation behavior of low-ash coking coal, Energy Sources, Part A: Recovery, Utilization, and Environmental Effects, 41 (5) (2019) 636–644.

[21] H. Wadell, *Volume, shape, and roundness of rock particles*, The Journal of Geology 40 (5) (1932) 443–451.

[22] R. D. Russell, R. E. Taylor, *Roundness and shape of Mississippi River sands*, The Journal of Geology 45 (3) (1937) 225–267.

[23] F. J. Pettijohn, Sedimentary rocks, Harper and Brothers, New York, 1949.

[24] M. C. Powers, *A new roundness scale for sedimentary particles*, Journal of Sedimentary Research 23 (1953) 117–119.

[25] N. A. Riley, *Projection sphericity*, Journal of Sedimentary Research 11 (2) (1941) 94–97.

[26] O. M. Longsworth, C. J. Bready, M. S. Joines, G. C. Shields, *The driving effects of common atmospheric molecules for formation of clusters: The case of sulfuric acid, nitric acid, hydrochloric acid, ammonia, and dimethylamine*, Environmental Science: Atmospheres 3 (2023) 1335–1351.

[27] C. Tsau, P. Lee, *Microstructures of Al7.5Cr22.5Fe35Mn20Ni15 high-entropy alloy and its polarization behaviors in sulfuric acid, nitric acid and hydrochloric acid solutions*, Entropy 18 (8) (2016) 288 12 pages.

[28] F. E. Critchfield, J. B. Johnson, *Differential, alkalimetric determination of sulfuric acid-hydrochloric acid and sulfuric acid-nitric acid mixtures*, Analytical Chemistry 26 (1954) 1803–1806.

[29] A. V. Dubenko, M. V. Nikolenko, O. Pasenko, A. Kostyniuk, B. Likozar, *Intensification of sulfuric acid leaching of altered ilmenite via adding fluoride activator*, Processes 9 (11) (2021) 1922 16 pages.

[30] Y. Mubarak, *Kinetics of hydrochloric acid leaching of copper from its ore*, International Journal of Emerging Trends in Engineering Research 8 (9) (2020) 5006–5015.

[31] A. Mukhachev, D. Yelatontsev, O. A. Kharitonova, *Physical and chemical foundations of the extraction refining of natural uranium*, Problems of Atomic Science and Technology 53 (25) (2022) 106–110.

[32] S. Teimouri, J. H. Potgieter, L. van Dyk, C. Billing, *The kinetics of pyrite dissolution in nitric acid solution*, Materials 15 (12) (2022) 4181 19 pages.

[33] A. Azizi, S. M. Ghasemi, *A comparative analysis of the dissolution kinetics of lead from low grade oxide ores in HCl, H2SO4, HNO3 and citric acid solutions*, Revue De Metallurgie-cahiers D Informations Techniques 114 (4) (2017) 406 12 pages.

[34] S. M. Ghasemi, A. Azizi, *Investigation of leaching kinetics of zinc from a low-grade ore in organic and inorganic acids*, I Journal of Mining and Environment 8 (2016) 579–591.

[35] B. E. Widyanto, S. W. Putri, *Corrosion behavior of ASTM A1008 carbon steel in mixtures of HNO3, H2SO4, and HCl using immersion and polarization methods*, Materials Transactions 60 (15) (2019) 732–736.

[36] Y. Ghorbani, J. Petersen, M. Becker, A. N. Mainza, J. P. Franzidis, *Investigation and modelling of the progression of zinc leaching from large sphalerite ore particles*, Hydrometallurgy 131-132 (2013) 8–23.

[37] N. A. Musunuri, P. Singh, I. S. Fischer, *PIV measurement of the transient fluid flow due to the adsorption of particles*, ASME 2014 4th Joint US-European Fluids Engineering Division Summer Meeting collocated with the ASME 2014 12th International Conference on Nanochannels, Microchannels, and Minichannels, Chicago, 2014, 10 pages.

[38] M. Wu, L. Xiong, J. Wang, *DEM study on effect of particle roundness on biaxial shearing of sand*, Underground Space 6 (6) (2021) 678–694.

[39] J. Li, Z. Wang, H. Xiu, X. Zhao, F. Ma, L. Liu, C. Yi, M. Zhang, E. Kozliak, Y. Ji, *Correlation between the powder characteristics and particle morphology of microcrystalline cellulose (MCC) and its tablet application performance*, Powder Technology 39 (2022) 117194 13 pages.

[40] K. R. Chu, E. Lee, S. H. Jeong, E. S. Park, *Effect of particle size on the dissolution behaviors of poorly water-soluble drugs*, Archives of Pharmacal Research 35 (2012) 1187–1195.